Biomass Conversion and Biorefinery
https://doi.org/10.1007/s13399-023-04192-y

ORIGINAL ARTICLE

Modeling and optimization of chemical-treated torrefaction of wheat straw to improve energy density by response surface methodology

Samuel Latebo Majamo[1] · **Temesgen Abeto Amibo**[2,3]

Received: 3 February 2023 / Revised: 3 April 2023 / Accepted: 10 April 2023

Abstract

Today, torrefaction is important technique for extending the potential of biomass for improvement of energy density. The independent variables investigated for torrefaction study were temperature, retention time, acid concentration, and particle size. The experiment was designed by central composite design (CCD) method using design expert (version 11). The three dependent variables were higher heating value (HHV), energy enhancement factor (EEF), and mass yield (MY) were carried out. Numerical optimization using response surface method (RSM) to maximize the HHV and EEF with lowest MY was carried out. The maximum HHV of 25.05MJ/kg, lowest MY of 60.15%wt and highest EEF of 1.593 were obtained at 299.99°C, 31.89min of retention time, 0.75g/l of acid concentration and 0.20mm of particle size. Proximate analysis, bulk density, hydrophobicity, energy density, and ultimate analysis of raw and torrefied biomass were determined to analyze the physiochemical properties of the fuel. In addition, thermo-gravimetric analysis (TGA), Fourier transform infrared spectroscopy (FTIR), and X-ray diffractometer (XRD) were done to distinguish the behavior of raw and torrefied wheat straw. The results implied that energy density of torrefied biomass was well improved when compared with raw biomass. All in all, energy density of torrefied biomass was improved, which can be used as an alternative energy.

Keywords Wheat straw · Chemical-treated torrefaction · Energy density · Optimization · RSM

1 Introduction

To meet the demand for a sustainable energy supply, it is necessary to develop a new alternative energy source that is renewable and sustainable, efficient, and economically viable. This is due to our dependence on fossil fuels for energy and the environmental consequences that result from their use [1–3]. Residual biomass is a carbon-neutral renewable resource that will play a significant role in the future as an alternative energy source. Wheat straw (WS) is a possible renewable and economically secure source of energy because it is an indigenous resource produced on a vast scale, is widely available around country side, and is very inexpensive [2, 4, 5].

Thus, increasing the energy from WS through the development of green and ecofriendly methods increases the added value of those waste materials. Torrefaction is a thermochemical pretreatment method that uses biomass at a limited temperature range value between 200 and 300°C [6]. Biomass undergoes torrefaction, which boosts its carbon per oxygen and carbon per hydrogen ratios and enhances its energy density [7–10]. The amount of fixed carbon in biomass rises following torrefaction as a result of charring of the biomass and cracking of volatiles. As hemicelluloses become more thermally stable and energy density rises with torrefaction temperature, the amount of fixed carbon increases following torrefaction [9, 10]. Today, torrefaction is perceived as a critical course for expanding the capability of biomass for huge scope creation of inexhaustible strong fuel with high energy density [11–13]. Torrefaction is a treatment process for biomass, which is

✉ Temesgen Abeto Amibo
temesgen.amibo@pg.edu.pl

[1] Department of Chemical Engineering, College of Engineering and Technology, Wachemo University, Hossana, Ethiopia

[2] Department of Process Engineering and Chemical Technology, Faculty of Chemistry, Gdansk University of Technology, Narutowicza 11/12, 80-233 Gdansk, Poland

[3] School of Chemical Engineering, Jimma Institute of Technology, Jimma University, P.O. Box-378, Jimma, Ethiopia

Published online: 26 April 2023

to reduce oxygen content and moisture absorption and increases the energy content [14, 15].

Dry and hydrothermal technologies for biomass torrefaction have been utilized extensively for many years [2, 16, 17]. Yet, according to the majority of the literatures, these traditional procedures were associated with low energy density, high moisture content, high O/C ratio, low hydrophobicity, low reactivity, and ignitability of torrefied biomass [5, 6]. Another method that was frequently utilized in reviews was the microwave assisted torrefaction [18]. These techniques' drawbacks include significant energy consumption, expensive, and the breakdown of the lignin, hemicellulose, and cellulose structures of torrefied biomass. As a result, the product would have lower heat content and higher ash content. These shortcomings in biomass torrefaction technology need the use of novel techniques that can reduce these shortcomings and enhance biomass torrefaction.

The chemical-treated torrefaction technique is preferred over traditional torrefaction techniques because of its significant benefits, including significant energy savings, increase in energy density, increase in calorific value, decrease in moisture content, decrease in the O/C ratio, an increase in reactivity, and an improvement in the ignitability of produced solid fuel. Because of chemical-treated torrefaction involves pre-treatment of raw material to improve the torrefied biomass fuel quality. Raw materials are initially pre-treated with highly diluted sulfuric acid to remove biomass impurities and improve raw materials. Unfortunately, biomass torrefaction has not yet adopted this cutting-edge chemically treated torrefaction method [19–22]. It is an incredible idea to combine this new torrefaction method with process condition optimization for biomass torrefaction.

In the current study, WS was torrefied utilizing a newly created chemically treated torrefaction procedure. The optimization of chemically treated biomass torrefaction has not been done in the previously reported literatures by taking into account significant process variables and numerous response variables [19–23] . The current analysis took into account the optimization of four crucial process factors that influence WS torrefaction with three responses in order to close these research gaps. In this study, the optimization process was designed and carried out using the RSM methodology of CCD. The study's objective was to increase energy density or Energy enhancement factor (EEF), by optimizing HHV at the lowest MY of torrefied biomass by applying chemical-treated torrefaction. It involved three levels of optimization of the following input parameters: temperature in the range of (200–300°C), retention time in the range of (30–60min), acid concentration in the range of (0.75-2.25g/l), and particle size in the range of (0.2–0.4mm). The physiochemical characteristics of the raw and torrefied biomass in current study were then identified and compared to published data.

2 Materials and methods

2.1 Materials

The raw material used for this study was WS which was taken from damping site as agricultural waste.

2.2 Chemicals and reagents

Sulfuric acid (98%), used to treat biomass in chemical torrefaction process, distilled water was used for washing the sample in order to remove the impurities from the biomass sample. Nitrogen gas was used during torrefaction to make the torrefaction environment inert. All chemicals and reagents used in this study were obtained from cherikos marketing center A.H plc., Addis Ababa, Ethiopia. All necessary materials used in present experiments were analytical graded. The equipment's used in this study were balance, oven, Muffle furnace, tubular Furnace with a stainless-steel tubular reactor, a glass reactor, different size conical and Erlenmeyer flasks, beakers, and measuring cylinders. Elemental analyzer (EA 1112 Flash CHNS-O- analyzer) powder X-ray diffractometer (XRD-7000), Fourier transform infrared spectroscopy (Spectrum 65 FT-IR, PerkinElmer), and thermo gravimetric analyzer (TGA) were used.

2.3 Methods

2.3.1 Biomass sample preparation and experimental design

Biomass sample preparation The pretreatment steps were adopted before the performing the experiments as reported literature [9]. WS was fractionated to remove the large (>4 mm) particles with the use of vibrating screen separator. Then, sample was washed by distilled water to remove impurities. Then it was kept in oven at 105°C for 30min. Then dried WS sample size was reduced to 0.2mm, 0.4mm, and 0. 6mm. The generalized torrefaction of WS process was described in Fig. 1.

2.4 Experimental design

From Table 1, the experiment was designed by CCD method. Four influential factors with three levels were designed as

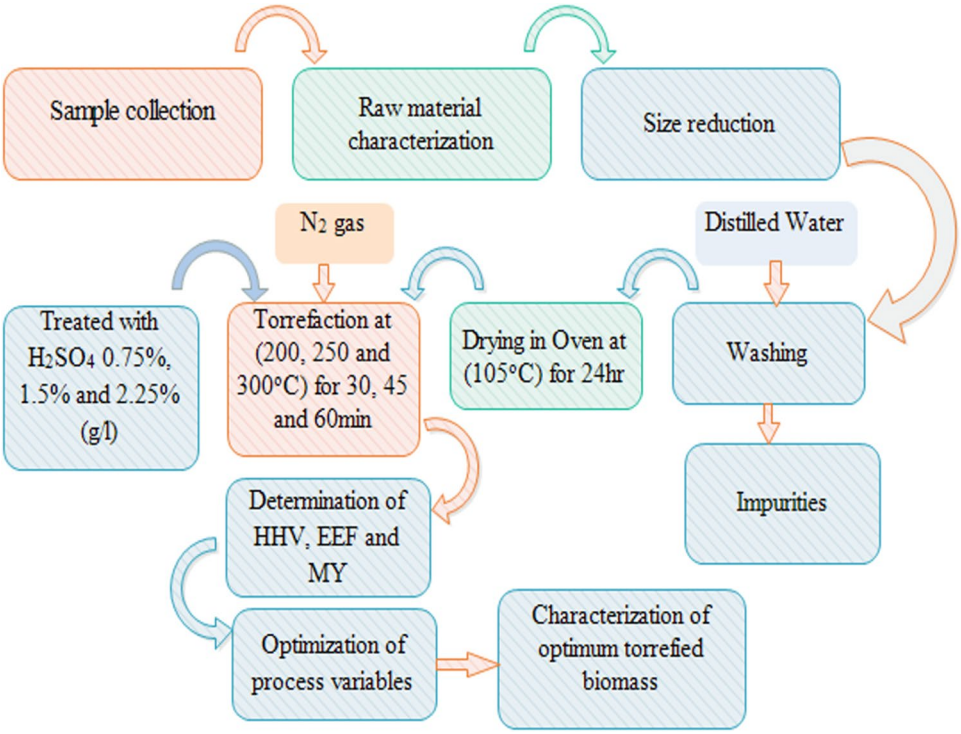

Fig. 1 General Experimental procedure of chemical-treated torrefaction

shown in Table 1. The sample size of WS taken for every torrefaction was 10±0.11gm.

2.4.1 Torrefaction process

A tubular reactor outfitted with a hot plate heater (AM 5250A), nitrogen cylinder, thermocouple, and pressure gauge was used for all experiments. A thermocouple was used to measure the reaction's temperature. To create an inert atmosphere, a valve was connected the reactor to a cylinder of 99.99% pure nitrogen gas that was flowing at a rate of 40 mL/min. The tubular reactor was filled with the samples and then completely purged with nitrogen gas to completely remove all oxygen. The reactor had been warmed at the set temperature for controlled residential time. The biomass samples were removed from the furnace after the prescribed amount of time had reached. In order to prevent moisture exposure, the samples were immediately placed in desiccators. The samples were weighed and put through the appropriate analysis after dried.

Table 1 Lower and upper limits designed by CCD

Factors	Lower limit	Upper limit
Torrefaction temperature (°C)	200	300
Retention time (min)	30	60
Acid concentration (g/l)	0.75	2.25
Particle size (mm)	0.2	0.6

2.4.2 Characterization of raw and torrefied biomass

Determination of moisture content 2±0.15g of raw or torrefied WS sample was weighed. The sample was placed in an oven and dried at 105°C for 2 h. After drying in the oven; the sample kept at desiccator for 30min. The weight of the sample was taken out every 10min. The procedure was repeated until a constant weight obtained. Three experiments were conducted. The average percentage of moisture content in the sample was determined using Eq. (1).

$$\%MC = \frac{W_1 - W_2}{W_1} * 100\%$$

$$Where, MC - moisture\ content\ of\ raw\ ortorrefied\ sample$$

$$W_1 - weight\ of\ sample\ drying, W_2 - weight\ of\ sample\ after\ drying \quad (1)$$

Determination of volatile content The percentage volatile content (VC %) was determined according to ASTM E 872 standard reported in literature [24]. The raw or torrefied WS sample weight of 2±0.15g was measured and recorded until a constant weight was obtained. Three samples were then kept in a furnace at a temperature of 550°C for 3h and weighed after cooling in desiccators. The average percentage volatile matter was then calculated using the Eq. (2)

$$\%VC = \frac{M_i - M_f}{M_i} * 100$$

$$Where, \%VC - percentage\ of\ volitle\ content$$

$$M_i - initial\ mass\ of\ sample, M_f - final\ mass\ of\ sample \quad (2)$$

Determination of the ash content Ash content determination was done according to the ASTM D2866-94 method suggested by [25]. A 15±0.15g sample in a standard condition was placed in to a porcelain crucible and transferred into a preheated muffle furnace set at a temperature of 1000°C and kept for 1 h. After that the sample was cooled and weighed. Three experiments were conducted. The average percentage ash content was determined using the Eq. (3)

$$\%Ash = \frac{M_{ash}}{M_i} * 100$$
$$Where, \%Ash - percentage\ of\ ash\ content$$
$$M_{ash} -, mass\ of\ ash, M_i - Initia\ mass\ of\ raw\ ortorrified\ sample \quad (3)$$

Determination of the fixed carbon Fixed carbon was determined by assuming that the sulfur content was negligible in all cases. The fixed carbon content (FC) was given in Eq. (4)

$$\%FC = 100\% - \%MC - \%VC$$
$$where, FC\ is\ fixed\ carbon(\%)\ , MC\ is\ Moisture\ Content(\%)$$
$$VC\ is\ Volatile\ Content(\%) \quad (4)$$

Elemental analysis Elemental analysis of the biomass samples were performed using an elemental analyzer (EA 1112 Flash CHNS-O- analyzer). 0.5±0.15gm of raw and torrefied WS sample was taken for elemental analysis. Conditions for the ultimate analysis were: Carrier gas flow rate of 120 ml/min, reference flow rate 100 ml/min, oxygen flow rate 250 ml/min; furnace temperature of 900°C and oven temperature of 75°C. Percentage of oxygen content was calculated by using Eq. (5)

$$Oxygen\% = Carbon\% - Hydrogen\% - Nitrogen\% - Ash\% \quad (5)$$

Determination of hydrophobic properties Hydrophobic property of torrefied and raw biomass was analyzed by equilibrium moisture content (EMC) analyzer. EMC was determined using Eq. (6)

$$\%EMC = \frac{M_e - M_d}{M_d} * 100$$
$$Where\ Me\ is\ the\ mas\ of\ the\ sample\ at\ equilibrium\ with\ a\ humid\ atmosphere\ and\ M_d\ is\ the\ mass\ o\ fdry\ sample.The\ sample\ was\ measured\ at\ 79\%\ relative\ humidity\ and\ temperature\ of\ 25°C \quad (6)$$

2.5 Determination of bulk density

Bulk density is the ratio of mass of biomass to the volume of water displaced. It was calculated using Eq. (7).

$$Densijty(g/ml) = \frac{mass\ of\ sample(g)}{volume\ of\ sample(ml)} \quad (7)$$

Higher heating value determination According to the ASTM D 3286 standard, the HHV of raw and torrefied samples were determined using bomb calorimeter (XRY-1A oxygen Bomb calorimetry) [26].

Mass yield (wt %) determination The products of torrefaction process were solid residue, condensable liquid (bio-oil) and non-condensable (NC) gases. The mass yield was calculated using Eq. (8).

$$Mass\ Yield(wt\%) = \frac{Wieght\ of\ torrefied\ biomass(g)}{Wieght\ of\ raw\ biomass(g)} \quad (8)$$

Energy yield (wt %) Energy yield (EY) is a function of solid product yield and their HHV. EY can be calculated using Eq. (9).

$$Energy\ Yeild(wt\%) = Mass\ yield * \frac{HHV_{TB}}{HHV_{RB}} * 100$$
$$Where, HHV_{TB} - is\ higher\ heating\ value\ of\ torrefied\ biomass$$
$$HHV_{RB} - is\ higher\ heating\ value\ of\ raw\ biomass \quad (9)$$

2.6 Energy enhancement factor /energy density

This indicates the potential calorific value of biomass. It was determined the correlation recommended by [24] using Eq. (10).

$$EEF(-) = \frac{HHV_{TB}}{HHV_{RB}}$$
$$Where, HHV_{TB} - is\ higher\ heating\ value\ of\ torrefied\ biomass$$
$$HHV_{RB} - is\ higher\ heating\ value\ of\ raw\ biomass \quad (10)$$

2.7 Thermo gravimetric analysis

Thermal stability of torrefied WS sample was determined by thermo gravimetric analyzer (TA instrument, model: SDT Q600). Thermal degradation of the sample was undergone starting from temperature of (27°C) up to upper limit temperature of 800°C with heating rate of 40.00°C/min under nitrogen atmospheric condition with flow rate

Table 2 Proximate analysis of raw wheat straw and other raw biomass

Raw biomass	Moisture content (%wt)	Volatile matter (%wt)	Fixed carbon content (%wt)	Ash content (%wt)	References
WS	5±0.1	59.4±0.03	27.3±0.02	7.9±0.04	This study
Food waste	11.95	81.0	3.77	3.28	[17]
Rice husk	8.8	59.2	14.6	26.2	[27]
Coffee husk	6.7	83.2	14	32.5	[27]

of 20.0 ml/min. The percent weight loss of the sample with corresponding temperature was determined.

2.8 FTIR characterization

FTIR spectroscopy (Spectrum 65 FT-IR, PerkinElmer) was used to determine the available functional groups and entire bonds of the raw and torrefied WS. The infrared spectra bands were recorded by passing of a beam of light through the solid sample at a resolution of $4cm^{-1}$ in the range of 4000 to $400cm^{-1}$. The differences among these samples in respective of associated functional groups were compared and discussed.

The powder X-ray diffractometer characterization The powder X-ray diffractometer (XRD-7000) was applied to determine the crystalline and amorphous structure of raw and torrefied biomasses. The XRD scans over the 2 θ in a range of 5–55°. The apparatus operated at current of 25mA and acceleration voltage of 30kv.

2.9 Numerical optimization

Numerical optimization will be carryout to identify the optimum condition which results in high calorific value with low mass yield by using numerical optimization feature of design expert software. The software manipulates the factors combinations that satisfy the requirements for responses and each of the factors. Three response variables (HHV, MY, and EEF) were determined and optimized.

3 Result and discussion

3.1 Raw material characterization

3.1.1 Proximate analysis

According to Mhilu [27], moisture content of raw rice husk and coffee husk are 6.7% and 8.8%, respectively, while in current study, moisture content is 5.01%; this implied that WS is more viable for torrefaction. The volatile content of WS in current study is comparable with moisture content of other biomasses of similar literatures [17, 27]. The raw WS possessed low moisture content and reasonable amount of volatile matter and fixed carbon that indicated that WS has potential to use as energy source. The results contributed to perform torrefaction to improve its energy. The experimental results were in good agreement with the reported studies as shown in Table 2.

3.1.2 Ultimate analysis

The ultimate analysis of raw WS possessed high carbon and oxygen content, and reasonable amount of hydrogen. According to Rasid et al. [17] and Mhilu [27], carbon content of sawdust and food waste is 43.55% and 44.61%, respectively; while in current study, carbon content of WS is 44% which is in reasonable agreement with the literatures. High carbon content biomass is recommended for torrefaction to improve energy [7]. In addition, in current experiment, sulfur content is 0.3% which is too low and cannot contribute any side effects at this amount. So, that WS can

Table 3 Ultimate analysis result of raw wheat straw and other raw biomass

Biomass	C	H	O	N	S	H/C	O/C	HHV (MJ/kg)	References
WS	44	5.8	42.4	0.4	0.3	0.13	0.96	15.72	This study
Sawdust	43.55	8.54	52.24	–	–	0.2	1.20	17.02	[27]
Food waste	44.61	7.34	44.16	3.48	0.4	0.166	0.99	19.67	[17]
Softwood	50.3	5.5	34.8	0.17	–	0.11	0.69	19.8	[7]
Peat pellets	52.8	5.2	37.4	1.17		0.098	0.708	20.9	[7]

Table 4 Responses of 3-level-4 factorial CCD design for torrefaction of wheat straw

Variables type:	Independent variables (factors)				Dependent variables (responses)		
Run	Temperature (^{o}C)	Time (min)	Acid concentration (g/l)	Particle size (mm)	HHV (MJ/kg)	MY (%wt)	EET (−)
1	300	30	0.75	0.2	25.05	59.34	1.59
2	250	45	1.5	0.4	22.65	81.72	1.44
3	300	30	2.25	0.2	23.01	64.45	1.46
4	300	60	0.75	0.2	21.30	58.72	1.35
5	300	30	0.75	0.6	17.50	77.92	1.11
6	250	45	1.5	0.6	18.40	89.42	1.17
7	200	60	2.25	0.6	17.80	73.53	1.13
8	200	30	0.75	0.2	22.20	73.43	1.41
9	200	60	2.25	0.2	20.20	76.63	1.28
10	200	30	2.25	0.2	20.70	85.45	1.32
11	250	45	1.5	0.4	22.02	82.32	1.4
12	250	45	0.75	0.4	24.03	81.32	1.53
13	250	60	1.5	0.4	18.60	74.32	1.18
14	250	45	1.5	0.4	22.43	81.32	1.43
15	200	30	0.75	0.6	17.43	92.63	1.11
16	200	30	2.25	0.6	16.08	81.86	1.02
17	300	60	0.75	0.6	17.50	77.63	1.11
18	300	30	2.25	0.6	18.20	62.86	1.16
19	250	45	2.25	0.4	22.01	79.32	1.4
20	300	60	2.25	0.6	18.65	64.82	1.18
21	200	60	0.75	0.2	21.05	62.35	1.34
22	250	30	1.5	0.4	20.24	82.64	1.29
23	200	60	0.75	0.6	19.04	83.73	1.21
24	250	45	1.5	0.4	21.92	82.34	1.39
25	250	45	1.5	0.2	23.40	81.32	1.49
26	250	45	1.5	0.4	21.83	83.32	1.39
27	300	45	1.5	0.4	22.97	69.53	1.46
28	300	60	2.25	0.2	20.93	64.53	1.33
29	250	45	1.5	0.4	21.67	82.54	1.38
30	200	45	1.5	0.4	22.05	83.21	1.4

Table 5 The ANOVA results of quadratic model for the correlations of HHV

Response 1: HHV						
Source	Sum of squares	df	Mean square	*F*-value	*p*-value	
Model	146.4	14	10.46	36.89	< 0.0001	Significant
A-temperature	4.07	1	4.07	14.36	0.0018	
B-time	1.58	1	1.58	5.59	0.032	
C-acid concentration	3.14	1	3.14	11.08	0.0046	
D-particle size	77.05	1	77.05	271.82	< 0.0001	
AB	3.12	1	3.12	10.99	0.0047	
AC	1.2	1	1.2	4.23	0.0575	
AD	1.35	1	1.35	4.75	0.0457	
BC	0.5184	1	0.5184	1.83	0.1963	
BD	7.92	1	7.92	27.96	< 0.0001	
CD	1.01	1	1.01	3.56	0.0786	
Lack of fit	3.54	10	0.3545	2.51	0.1611	Not significant

Table 6 The ANOVA results of quadratic model for the correlations of MY

Response 2: mass yield						
Source	Sum of squares	df	Mean square	*F*-value	*p*-value	
Model	2407.93	14	172	166.18	< 0.0001	Significant
A-temperature	709.64	1	709.64	685.65	< 0.0001	
B-time	109.13	1	109.13	105.44	< 0.0001	
C-acid concentration	10.31	1	10.31	9.96	0.0065	
D-particle size	339.56	1	339.56	328.08	< 0.0001	
AB	91.49	1	91.49	88.4	< 0.0001	
AC	31.02	1	31.02	29.98	< 0.0001	
AD	0.3306	1	0.3306	0.3194	0.5803	
BC	2.09	1	2.09	2.02	0.176	
BD	1.49	1	1.49	1.44	0.249	
CD	462.9	1	462.9	447.25	< 0.0001	
Lack of fit	13.14	10	1.31	2.75	0.1377	Not significant

be used as energy source. The experimental results were in good agreement with the reported studies as shown in Table 3.

3.2 Experimental and ANOVA results

The independent factors and dependent variables were represented in Table 4. The experiments were conducted according to randomly displayed run order designed by designed expert version-11 software. ANOVA results of quadratic models for determination of HHV, MY and EEF were represented in Table 5, Table 6, and Table 7 respectively.

Fit summary of the quadratic model for dependent variables (HHV, MY and EEF) was shown in Table 8. The adequacy of the model was evaluated by *F*-value, lack of fit, *P*-value, and coefficients of determination. The adequacy of the established model was further supported by high value of coefficient of determination terms: R^2 value of 0.9718, 0.9936, and 0.9718 for HHV, MY, and EEF respectively. The coefficient terms with *P*-value greater than 0.05 are not significant, whereas *P*-values less than 0.0500 indicate model terms are significant. Coefficient of variation of all three response parameters indicated that model was matched with experimental data.

Internal studentized residual is used to check goodness of data fit on regression line under suggested model. In Fig. 2, all the residuals were fitted on linear line. This implies that data was well fitted with experimental results and is possible to predict the response parameters.

Figure 3 represented that the actual verse predicted value of HHV, MY, and EEF. These linear lines drown at 45° indicated that the actual and predicted values of response variables were closer to each other. This implies that experimental data was in reasonable agreement with suggested quadratic model, which means data was well with model to predict response parameters at given range values. The equation in terms of coded factors is an important to determine the influence of process parameters by comparing the

Table 7 The ANOVA results of quadratic model for the correlations of EEF

Response 3: EEF						
Source	Sum of squares	df	Mean square	*F*-value	*p*-value	
Model	0.5924	14	0.0423	36.89	< 0.0001	Significant
A-temperature	0.0165	1	0.0165	14.36	0.0018	
B-time	0.0064	1	0.0064	5.59	0.032	
C-acid concentration	0.0127	1	0.0127	11.08	0.0046	
D-particle size	0.3118	1	0.3118	271.82	< 0.0001	
AB	0.0126	1	0.0126	10.99	0.0047	
AC	0.0049	1	0.0049	4.23	0.0575	
AD	0.0054	1	0.0054	4.75	0.0457	
BC	0.0021	1	0.0021	1.83	0.1963	
BD	0.0321	1	0.0321	27.96	< 0.0001	
CD	0.0041	1	0.0041	3.56	0.0786	
Lack of fit	0.0143	10	0.0014	2.51	0.1611	Not significant

Table 8 Fit summary of the quadratic model for HHV, MY, and EEF

Fit summary	HHV	Mass Yield	EEF
R-square	0.9718	0.9936	0.9718
Adjusted ***R***-square	0.9454	0.9876	0.9454
Predicted ***R***-square	0.8445	0.9666	0.8445
Adequacy precision	22.7767	48.4645	22.7767
Sequential ***P***-value	< 0.0001	< 0.0001	< 0.0001
Std. dev.	0.5324	1.02	0.0339
Mean	20.7	76.48	1.32
Coefficient of variation %	2.57	1.33	2.57

parameters coefficients. By ignoring non-significant factors and interaction of factors, the HHV, MY, and EEF can be determined by using coded equation Eq. (11), Eq. (12), and Eq. (13) respectively.

$$HHV(Mj/Kg) = 22.06 + 0.4756A - 0.2967B - 0.4178C - 2.07D - 0.4412AB - 0.29AD + 0.7038BD + 0.4795A^2 - 2.61B^2 - 1.13D^2 \quad (11)$$

$$MY(\%) = 82.44 + A - 6.28B - 0.7567C + 4.43D + 2.39AB - 1.39AC - 5.38CD - 6.25A^2 - 4.14B^2 - 2.30C^2 + 2.75D^2 \quad (12)$$

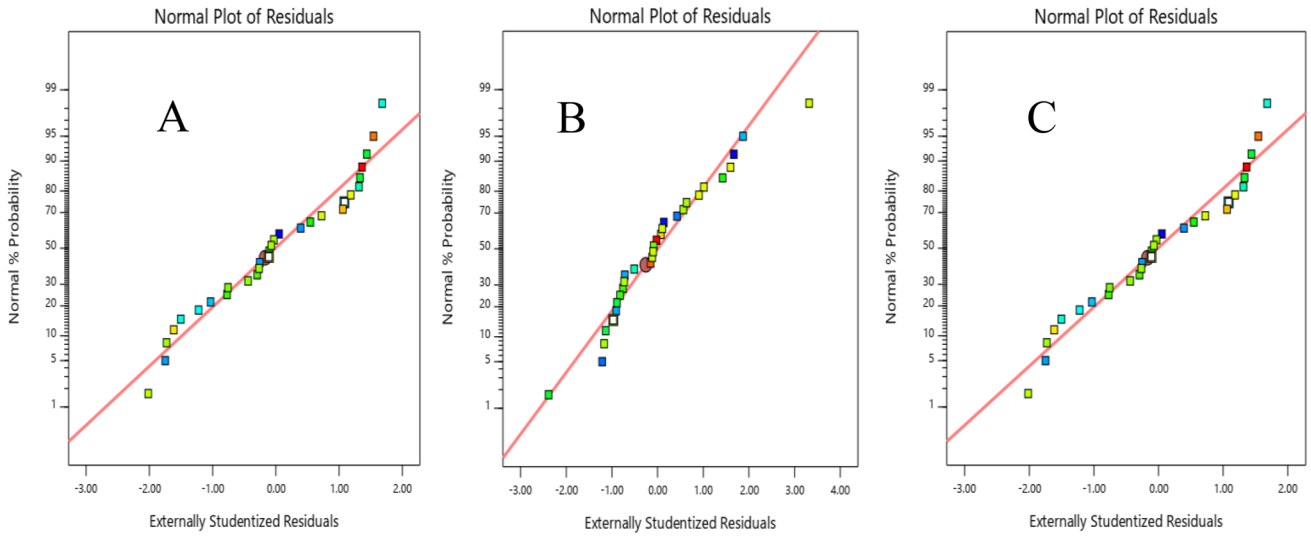

Fig. 2 Normal plot of residuals for **A** HHV, **B** MY, and **C** EEF of the torrefaction.

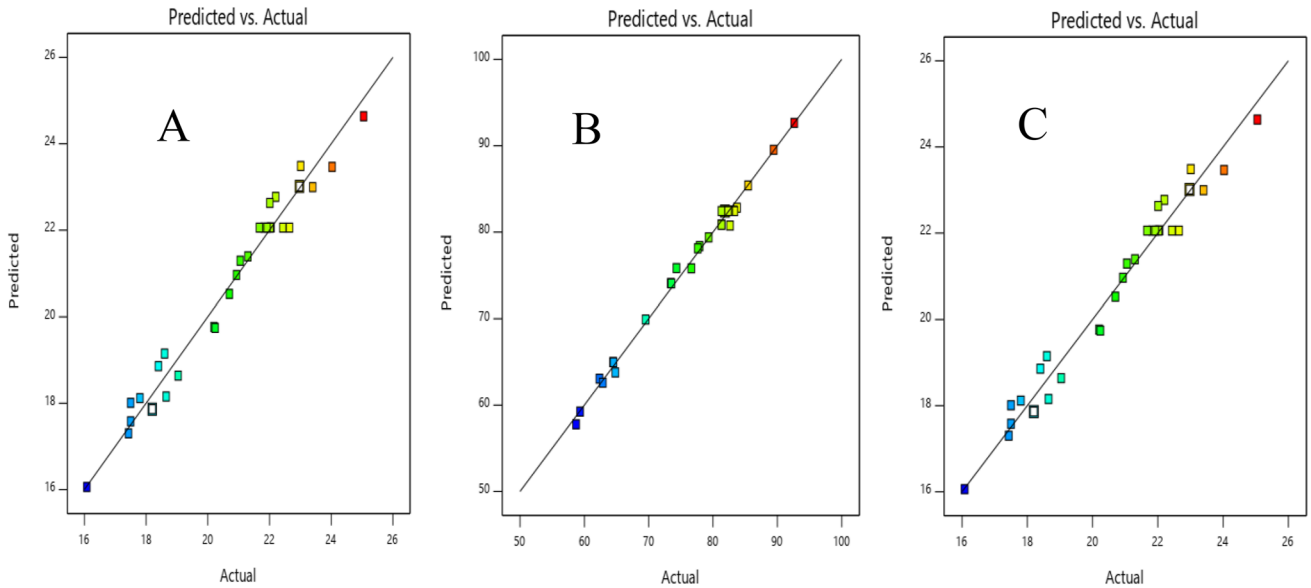

Fig. 3 Predicted verses actual responses of **A** HHV, **B** MY, and **C** EEF of torrefaction

$$EEF(-) = 1.40 + 0.0303A - 0.0189B - 0.0266C - 1316D - 0.0281AB - 0.0184AD + 0.0448BD + 0.0305A^2 - 1661B^2 + 0.0629C^2 - 0.0719D^2 \quad (13)$$

where; $A - torrefaction\ temperature(^{\circ}C), B - retention\ time(min)$
$C - acid\ concentration(g/l)\ and\ D - particle(mm)$

3.3 Single and interaction effects of process variables

Three responses were used to study and compare the effect of process conditions on torrefaction process. All single factors; temperature (A), time (B), acid concentration (C), and particle size (D) had significant effect on torrefaction process. As torrefaction temperature increased, the HHV also increased while MY decreased. Low particle size and acid concentration resulted in maximum HHV. This is because of small particles can store energy, since specific surface area to store kinetic energy is high. The independent variables effect in this study is in reasonable agreement with similar literatures [28]. A^2 harmed the HHV and EEF. This is because, at double temperature, the energy containing molecules damaged. The 3D surface plots show the effect of any two process conditions on individual responses, keeping the third condition at mid-point was investigated. Figure 4 indicates the interaction effect of process variables on HHV and EE. Figure 5 indicates the interaction effect of process variables on MY. These plots make it possible to study how each response changes while varying process conditions simultaneously, i.e., avoiding considering one factor at a time.

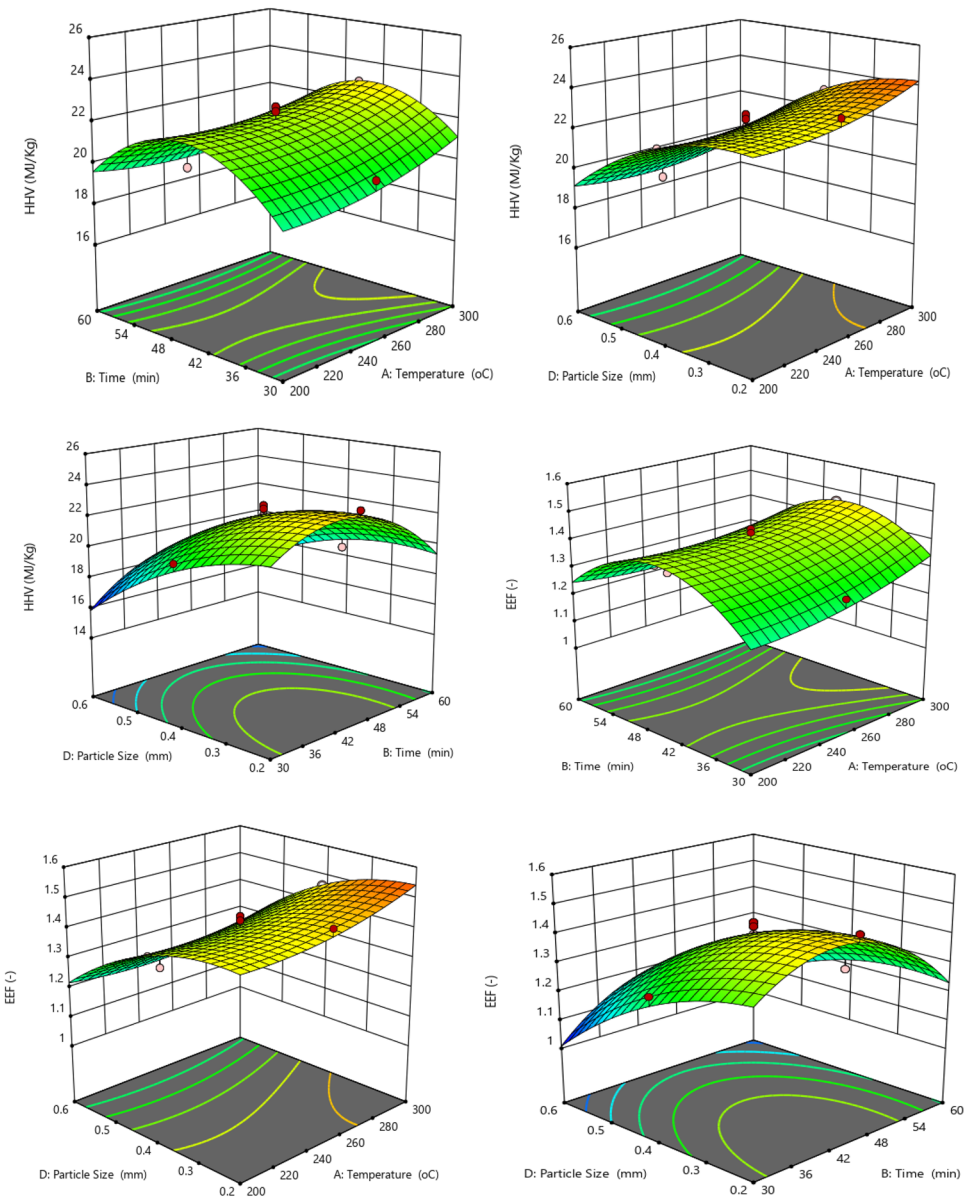

Fig. 4 Interaction effects of process variables on HHV and EEF of torrefied process

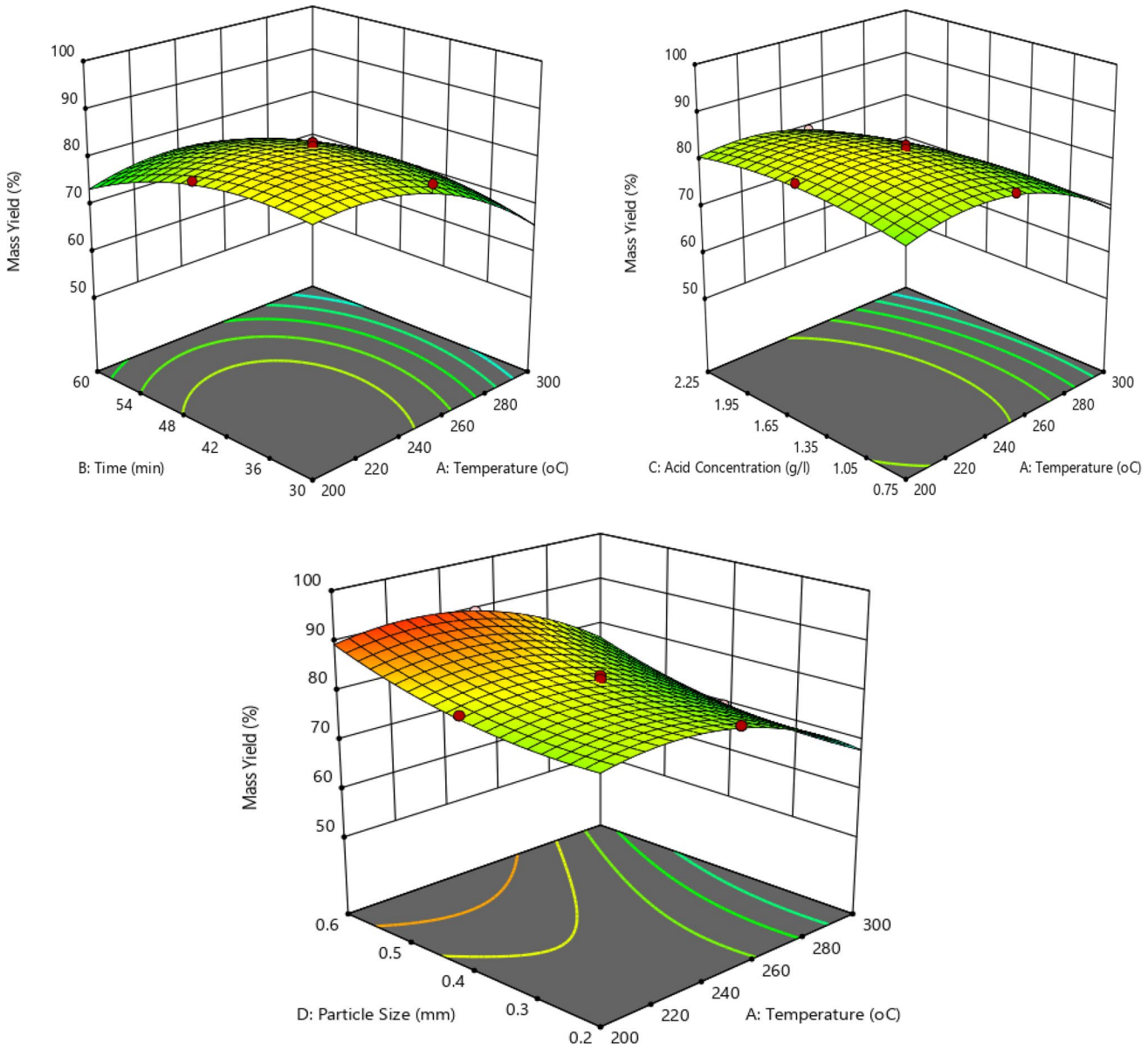

Fig. 5 Interaction effects of process variables on MY of torrefaction process

3.3.1 The effect of process conditions on higher heat value and energy enhancement factor

As temperature increased, the HHV increases also. Increment in temperature has positive effect. The same is true for EEF. The combined parameters effect on HHV was shown in Figure 4. It is shown that the HHV of biomass is highly significantly (i.e., P <0.0001) influenced by the reaction temperature, particle size, retention time and acid concentration. As temperature and retention time

Table 9 Proximate analysis result of torrefied WS and another torrefied biomass

Torrefied biomass	Moisture content (%wt)	Volatile matter (%wt)	Fixed carbon content (%wt)	Ash content (%wt)	References
WS	2.02	33.04	47.56	17.3	This study
Acacia nilotica	1.67	44.78	52.13	1.42	[30]
Poultry litter	–	47.12	25.02	30.13	[31]
Digested sewage sludge	–	54.26	19.48	19.28	[31]

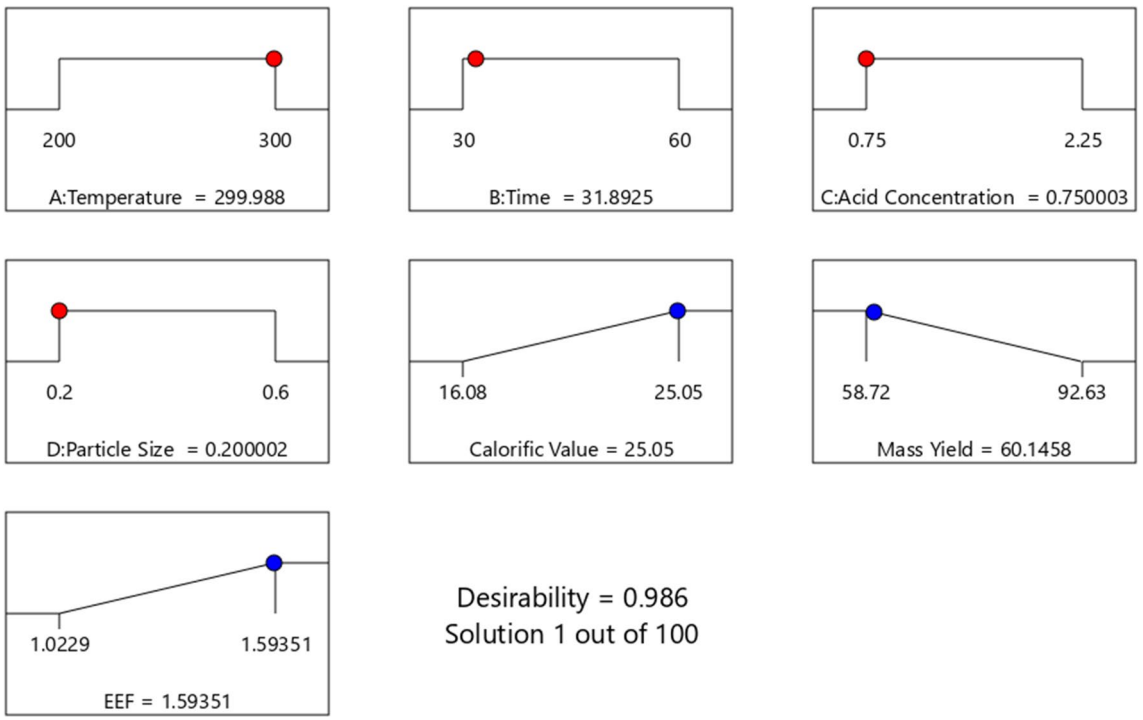

Fig. 6 All the factors and responses with their constraint of optimization criteria

increased, HHV increased. Further, Increment of these two variables decreased the HHV and EEF. This is due to breaking of heat storing molecules of biomass. At middle value of both variables resulted in maximum HHV and EEF. This was conformed to reported literature [12].

3.3.2 The effect of process conditions on mass yield

The graphical representation of the effect of process conditions on the mass yield of fuel is shown in Figures 5 during torrefaction. It was observed that in increment of torrefaction temperature, retention time and acid concentration, the mass loss of biomass fuel was increased. This is due to the methoxy group removal from the lignin part of wheat straw and end of the carboxyl group from the WS hemicellulose [25]. When acid concentration increased with increasing time, mass loss increased. As acid concentration increased, biomass loses its amorphous structure which lead to decrease in weight.

The evacuation of both the carbonyl and carboxyl components from the cellulose part of WS could likewise be reasons for the mass loss. But, in an increment of particle size, the mass loss of biomass fuel decreased. This indicates that lignin, cellulose, and hemicellulose of biomass sample having large particle size cannot be easily destructed. This was supported by reported research [29].

3.4 Optimization of process conditions

In current study, optimization was pinned because the aim of the study is to identify the best process condition suitable to perform torrefaction. To increase the HHV and EEF, and to decrease the MY of the biomass, numerical optimization was performed. The best identified conditions of four factors such reaction temperature, acid concentration, reaction time, and catalyst weight were determined by design expert software feature of RSM. The software displayed the best condition which can result in maximum HHV and minimum

Table 10 Ultimate analysis result of torrefied WS and another torrefied biomass

Biomass	C	H	O	N	S	H/C	O/C	HHV (MJ/kg)	References
WS	65.44	3.05	31.05	0.05	0.03	0.05	0.47	25.05	This study
Soft wood	51.93	6.53	26.07	0.41	-	0.126	0.50	22.12	[28]
Rice husk	66.76	3.12	23.89	1.775	0.75	0.047	0.358	22.5	[32]
Corncob	81.56	3.84	4.82	8.32	1.46	0.047	0.059	19.5	[32]

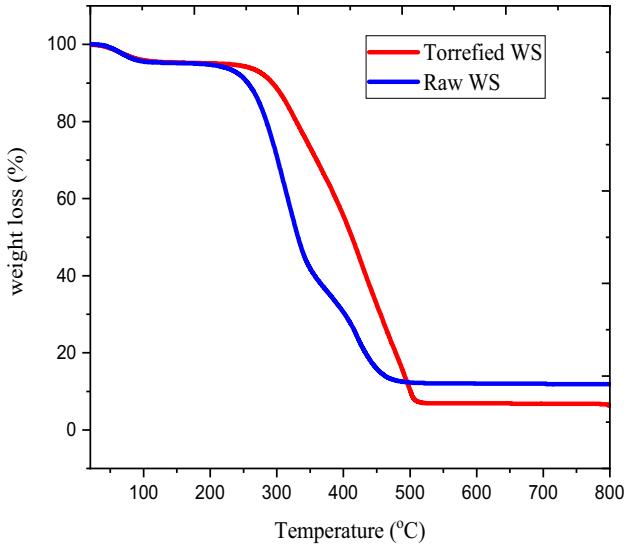

Fig. 7 TGA curves for raw wheat straw and torrefied wheat straw

MY. The four factors and three responses with their criteria were available in Fig. 6. The best torrefaction condition was identified and suggested by software.

The validation of model was carried out through experimentation. The obtained condition was then evaluated by conducting triplicate experiments and composite desirability. The maximum desirability given by software was 0.986 which was much closer the maximum value (1). This indicates that the obtained optimum variables condition was interesting. In addition, the average values of triplicate experiment results of HHV, MY, and EEF were 25.03MJ/kg, 60.02%w/w, and 1.59224 respectively. There was too small difference in experimental values and the predicted values suggested by software. This indicates that suggested model and experiments were well fitted. This result is good when compared with dry torrefied WS reported in literature [29].

3.5 Characterization results of optimum torrefied wheat straw

3.5.1 Proximate analysis

The proximate analysis result of torrefied WS showed significant change from the raw WS. Reduction in moisture content observed. In addition, small amount of light volatile matter released and its fixed carbon content increased. The results were conformed to literatures as shown in Table 9. As summarized in Table 9, according to Singh et al. [30], volatile matter and fixed carbon contents are 44.78% and 52.13% which are comparable to current study having 33.04% and 47.56% for volatile content and fixed carbon respectively. Torrefied biomass having high volatile matter and fixed carbon are recommended fuel, because they contain high amount of energy and the life time during burning is also high [30]. In contrast, according to Barskov et al. [31], fixed carbon content of poultry litter and digested sewage sludge are low when compared to present study. Torrefied biomass having low fixed carbon cannot be thermally stable, since which resulted in high amount of ash content.

3.5.2 Ultimate analysis

The elemental analysis of torrefied WS in Table 10 shows that the content of carbon increased as a result of torrefaction while the content of hydrogen and oxygen were decreased. According to Mukhtar et al. [32], carbon content of rice husk and corncob are 66.76% and 81.56% respectively. While in according to Lee et al. [11], carbon content of softwood is 51.93%. In current study carbon content is 66.44% which is comparable result with reported literatures summarized in Table 10. As the result of a change in chemical composition, the atomic ratio of O/C and H/C of the torrefied WS are 0.47 and 0.05 respectively, which are low in comparison to raw WS. This is due to the release of volatile-rich in hydrogen and oxygen, such as water, carbon mono oxide, and carbon dioxide during torrefaction [33]. There is low nitrogen and sulfur detected in torrefied WS.

3.5.3 Hydrophobicity and bulk density

A significant amount of oxygen was removed, and the hydroxyl groups in the hemicelluloses were broken, according to the EMC result of the current experiment, which is shown in Table 10. Torrefied WS become more hydrophobic as a result of the dissolution of these hydroxyl groups after torrefaction. Torrefaction replaces OH groups with non-polar groups, which gives the torrefied biomass its hydrophobic properties. Due to this, even in damp storage environments, the torrefied product is less prone to biodegradation, moisture uptake, and self-ignition [25]. Bulk density of torrefied biomass was lower than that of raw biomass for hydrothermal torrefaction. Nonetheless, the bulk density of torrefied biomass is higher than raw biomass in the case of dry torrefaction. In the current experiment as shown in Table 11, torrefied WS was denser than raw WS. This was accomplished by properly pretreating the material in the current study. This demonstrates that torrefied WS occupied little area while having its mass.

Table 11 Hydrophobicity and bulk density of raw and torrefied WS

Biomass	Equilibrium moisture content (%)	Bulk density (kg/m^3)
Raw WS	5.3± 0.02	160± 0.07
Torrefied WS	2.1± 0.04	172± 0.04

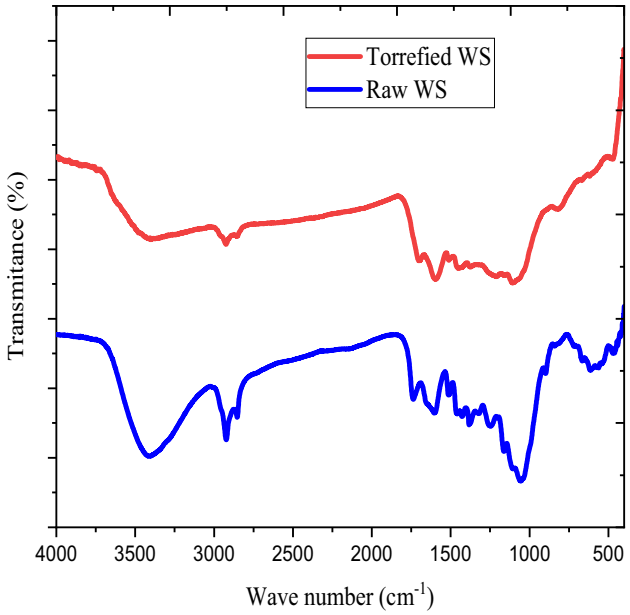

Fig. 8 FTIR spectrum of raw and torrefied wheat straw

3.6 Thermo gravimetric analysis

The TGA curves of raw and torrefied WS presented were in Fig. 7. It involved three main stages: initial stage (<200°C), destruction/devolatilization stage (250−510°C), and char/ash formation stage (>500°C). For both samples, it was observed that an initial low weight loss occurs in the range of 35–200 °C, due to the removal of adsorbed moisture and low molecular weight volatile matters. TGA curve of raw WS showed rapid weight loss from 250 to 510°C; this indicates that removal of untreated light solid particles and destruction of hemicellulose and cellulose. While in torrefied WS, removal of untreated light solid matters has not been observed, owning sample was well treated with dilute H_2SO_4. By other word, unnecessary material which affects torrefaction process was removed at treatment stage. But, destruction of hemicellulose and cellulose has been observed at 253–510°C. This was in agreement with literature[30]. From 510 to 800°C, it was observed that very small weight loss in both samples. This was due to the decomposition of lignin. Similar report was reported in [33]. In Fig. 7, as TGA profile indicating, residue of torrefied sample was lower than that of raw sample. This indicates that torrefied sample resulted in low ash formation after firing that was the result of treatment. As a whole, TGA curve of chemical-treated torrefied WS was good, so it can be useful fuel.

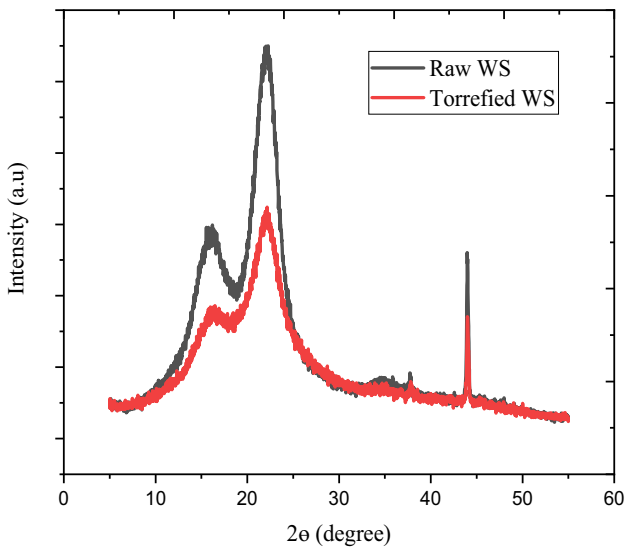

Fig. 9 XRD diffraction peak patterns of raw and torrefied wheat straw

3.7 FTIR analysis

Figure 8 shows the FTIR spectrum of raw and torrefied WS to examine the entire bond and functional groups. In a raw biomass, a strong O–H stretching absorption was observed at 3329 cm^{-1} and C–H stretching absorption at 2909 cm^{-1} can indicates the aliphatic chain [34]. There are many clear peaks observed in the region in between 1750 cm^{-1} and 1000 cm^{-1} in raw WS. The peaks at 1732 cm^{-1} associated for unconjugated C=O in hemicellulose. The associated peaks at 1630−1645 cm^{-1} and 1400−1510 cm^{-1} indicate C=C vibration peaks of benzene ring in lignin. Stretching vibration peaks at 1210−1255 cm^{-1} is assigned to C-O stretching in lignin [35]. Strong peak of raw WS at 1000cm^{-1} is the peak of the C−O bond in hemicellulose and cellulose. The peak at 785 cm^{-1} indicates wagging vibrations of C-H in cellulose [34].

After torrefaction, the peak at 3329 cm^{-1} indicating O-H band was weakened. The decrease in peak intensity indicates that the hydroxyl group almost disappeared after torrefaction. This was due to loss of water in torrefied biomass [36–38]. The adsorption of C−H bond at 2909 cm^{-1} also weakened. This indicates that during the torrefaction process, the demethylene reactions and demethylation occurred to the glucose unit in cellulose and xylan unit in hemicellulose, resulting in the decrease of C−H [37]. Its disappearance explains disruption of cellulose and hemicellulose. The aliphatic chain can produce C_2H_6, C_2H_4, and CH_4 in gaseous products. The at 1000cm^{-1} in raw WS shifted to 970cm^{-1} in torrefied WS and almost disappeared, which clearly shows that when torrefaction is carried out, decarboxylation reactions occurred in cellulose. The FTIR analysis results of current study were in agreement with reported literatures[31–33]. All the structural changes observed in torrefied WS is due to de-oxidation process, and can be applied for efficient use for energy generation.

3.8 XRD analysis

The XRD diffraction patterns of raw and torrefied WS represented in Fig. 9. It showed similar XRD diffraction peak patterns, indicating that oxidative torrefaction had no significant effect on the crystal type of the biomass. The diffraction angle (2θ) at 16.10−16.30° can indicate amorphous phase. The diffraction angles (2θ) at 21.90−22.30° and 44.5–50° can indicate crystallographic phase [37]. The peak appearing at 16.10−16.30° decreased in torrefied WS, which indicates destruction of cellulose and increment of crystallinity. This can result in low ash content in torrefied biomass in large thermal stability. The result of current study is in good agreement with other results of present study and reasonable agreement with similar reported literatures[32, 33].

4 Conclusion

Optimization of chemical-treated torrefaction to maximize HHV and (EEF) with lowest MY was carried out. The 3-level 4-factors (torrefaction temperature, retention time, acid concentration, and particle size) experiment was designed by central composite design (CCD) method. Numerical optimization was carried out using RSM with three response variables HHV, MY, and EEF. The maximum HHV of 25.05MJ/kg, lowest mass yield of 60.15%wt, and maximum EEF of 0.20 were obtained at 299.99°C, 31.89min, 0.75g/l H_2SO_4, and 0.20mm of particle size. Proximate analysis, hydrophobicity, ultimate analysis, bulk density, and energy density of raw and torrefied WS were determined. As temperature increased, HHV, energy density, and bulk density increased while MY decreased. TGA, FTIR, and XRD resulted indicated that torrefied biomass was good when compared to raw biomass. In view of the results obtained in this article, the torrefied WS has a potential to be used as a source of alternative energy.

5 Recommendations

It is better if future research carried out the optimization using general factorial design to compare with present work results and conducted all the physiochemical properties and compared with latest reported work on different biomass.

6 Limitations

Some limitations happened during conducting this work, such as: lack of scanning electron microscopy to analysis the detail microstructure of the raw and torrefied sample.

Acknowledgements The authors would like to thank the Department of Chemical Engineering, Wachemo University, Hossana.

Data availability The data used to support the findings of this study are included in the article.

Declarations

Ethics approval and consent to participate Not applicable.

Consent for publication Not applicable.

Competing interests The authors declare no competing interests.

References

1. Batidzirai B, Mignot APR, Schakel WB, Junginger HM, Faaij APC (2013) Biomass torrefaction technology: techno-economic status and future prospects. Energy 62:196–214. https://doi.org/10.1016/j.energy.2013.09.035
2. Nhuchhen D, Basu P, Acharya B (2014) A comprehensive review on biomass torrefaction. Int J Renew Energy Biofuels 2014:1–56. https://doi.org/10.5171/2014.506376
3. Tripathi N, Hills CD, Singh RS, Atkinson CJ (2019) Biomass waste utilisation in low-carbon products: harnessing a major potential resource. NPJ Clim. Atmos Sci 2(1):35. https://doi.org/10.1038/s41612-019-0093-5
4. Chen Z, Wang M, Ren Y, Jiang E, Jiang Y, Li W (2018) Biomass torrefaction: a promising pretreatment technology for biomass utilization. IOP Conf Ser Earth Environ Sci 113(1):012201. https://doi.org/10.1088/1755-1315/113/1/012201
5. Sakkour AN, Al-Abdullah AM (2020) Torrefaction of wheat straw. Am J Eng Res 9(5):185–190. [Online]. Available: www.ajer.org
6. Satpathy SK, Tabil LG, Meda V, Naik SN, Prasad R (2014) Torrefaction of wheat and barley straw after microwave heating. Fuel 124:269–278. https://doi.org/10.1016/j.fuel.2014.01.102
7. Andersone A, Arshanitsa A, Akishin Y, Semenischev A (2019) Microwave assisted torrefaction of plant biomass of different origin with a focus on solid products valorisation for energy and beyond. Chem Eng Trans 86:109–114. https://doi.org/10.3303/CET2186019
8. Chen W-H, Lu K-M, Lee W-J, Liu S-H, Lin T-C (2014) Non-oxidative and oxidative torrefaction characterization and SEM observations of fibrous and ligneous biomass. Appl Energy 114:104–113. https://doi.org/10.1016/j.apenergy.2013.09.045
9. Mosqueira D et al (2018) CRISPR / Cas9 editing in human pluripotent stem cell-cardiomyocytes highlights arrhythmias,

hypocontractility, and energy depletion as potential therapeutic targets for hypertrophic cardiomyopathy. Eur Heart J 44:3879–3892. https://doi.org/10.1093/eurheartj/ehy249
10. Nhuchhen DR (2016) Prediction of carbon, hydrogen, and oxygen compositions of raw and torrefied biomass using proximate analysis. Fuel 180:348–356. https://doi.org/10.1016/j.fuel.2016.04.058
11. Song K et al (2012) Precipitation of calcium carbonate during direct aqueous carbonation of flue gas desulfurization gypsum. Chem Eng J 213:251–258. https://doi.org/10.1016/j.cej.2012.10.010
12. Mohamed AR, Nadhirah N, Nordin A, Hasyierah N, Salleh M (2019) Chemical properties of torrefied and raw sawdust. J Adv Res Eng Knowl 6:7–14.
13. Sulaiman MH, Uemura Y, Azizan MT (2016) Torrefaction of empty fruit bunches in inert condition at various temperature and time. Procedia Eng 148:573–579. https://doi.org/10.1016/j.proeng.2016.06.514
14. Wilk M, Magdziarz A, Kalemba I, Gara P (2016) Carbonisation of wood residue into charcoal during low temperature process. Renew Energy 85:507–513. https://doi.org/10.1016/j.renene.2015.06.072
15. Zheng A et al (2015) Comparison of the effect of wet and dry torrefaction on chemical structure and pyrolysis behavior of corncobs. Bioresour Technol 176:15–22. https://doi.org/10.1016/j.biortech.2014.10.157
16. Pelaez-Samaniego MR, Yadama V, Garcia-Perez M, Lowell E, McDonald AG (2014) Effect of temperature during wood torrefaction on the formation of lignin liquid intermediates. J Anal Appl Pyrolysi 109:222–233. https://doi.org/10.1016/j.jaap.2014.06.008
17 Rasid RA, Chin TM, Ismail M, Rahman RNUA (2019) Effect of torrefaction temperature, residence time and particle size on the properties of torrefied food waste. Indones J Chem 19(3):753–760. https://doi.org/10.22146/ijc.39718
18 MohdFuad MAH, Hasan MF, Ani FN (2019) Microwave torrefaction for viable fuel production: A review on theory, affecting factors, potential and challenges. Fuel 253:512–526. https://doi.org/10.1016/j.fuel.2019.04.151
19. Chen D, Cen K, Cao X, Li Y, Zhang Y, Ma H (2018) Restudy on torrefaction of corn stalk from the point of view of deoxygenation and decarbonization. J Anal Appl Pyrolysis 135(July):85–93. https://doi.org/10.1016/j.jaap.2018.09.015
20. Prakash Kumar BG et al (2019) Torrefied materials derived from waste vegetable biomass. Mater Today Proc 28(xxxx):852–855. https://doi.org/10.1016/j.matpr.2019.12.311
21. Chen C, Qu B, Wang W, Wang W, Ji G, Li A (2021) Rice husk and rice straw torrefaction: properties and pyrolysis kinetics of raw and torrefied biomass". Environ Technol Innov 24(101872):2021. https://doi.org/10.1016/j.eti.2021.101872
22. Acharya B, Dutta A, Minaret J (2015) Review on comparative study of dry and wet torrefaction. Sustain Energy Technol Assessments 12:26–37. https://doi.org/10.1016/j.seta.2015.08.003
23. Adhikari BB et al (2019) Pelletization of torrefied wood using a proteinaceous binder developed from hydrolyzed specified risk materials". Processes 7(4):1–12. https://doi.org/10.3390/pr7040229
24. Aytenew G, Nlgus G, Bedewi B (2018) Improvement of the energy density of rice husk using dry and chemical treated torrefaction. J Adv Chem Eng 08(01):4–9. https://doi.org/10.4172/2090-4568.1000185
25. Pahla G, Ntuli F, Muzenda E (2018) Torrefaction of landfill food waste for possible application in biomass co-firing. Waste Manag 71(2017):512–520. https://doi.org/10.1016/j.wasman.2017.10.035
26. Chin KL et al (2013) Optimization of torrefaction conditions for high energy density solid biofuel from oil palm biomass and fast growing species available in Malaysia. Industrial Crops Products 49:768–774. https://doi.org/10.1016/j.indcrop.2013.06.007
27. Mhilu CF (2014) Analysis of energy characteristics of rice and coffee husks blends. Chem Eng 2014:1–6. https://doi.org/10.1155/2014/196103
28. Lee J-W, Kim Y-H, Lee S-M, Lee H-W (2012) Bioresource Technology Optimizing the torrefaction of mixed softwood by response surface methodology for biomass upgrading to high energy density. Bioresour Technol 116:471–476. https://doi.org/10.1016/j.biortech.2012.03.122
29. Ikegwu UM, Ozonoh M, Okoro NJM, Daramola MO (2021) Effect and optimization of process conditions during solvolysis and torrefaction of pine sawdust using the desirability function and genetic algorithm. ACS Omega 6(31):20112–20129. https://doi.org/10.1021/acsomega.1c00857
30. Singh S, Chakraborty JP, Mondal MK (2019) Optimization of process parameters for torrefaction of Acacia nilotica using response surface methodology and characteristics of torrefied biomass as upgraded fuel. Energy 186:115865. https://doi.org/10.1016/j.energy.2019.115865
31. Barskov S et al (2019) Torrefaction of biomass : A review of production methods for biocoal from cultured and waste lignocellulosic feedstocks. Renew Energy 142:624–642. https://doi.org/10.1016/j.renene.2019.04.068
32. Mukhtar H, Feroze N, Munir HMS, Javed F, Kazmi M (2020) Torrefaction process optimization of agriwaste for energy densification. Energy Sources. Part A Recover Util Environ Eff 42(20):2526–2544. https://doi.org/10.1080/15567036.2019.1609626
33 Fuelbiol F, Wang L, Hong J, Ren J, Du F, Hu J (2015) The impact of glycerol organosolv pretreatment on the chemistry and enzymatic hydrolyzability of wheat straw Bioresource Technology The impact of glycerol organosolv pretreatment on the chemistry and enzymatic hydrolyzability of wheat straw. Bioresour Technol 187(2018):354–361. https://doi.org/10.1016/j.biortech.2015.03.051
34. Aslam U, Ramzan N, Aslam Z, Iqbal T (2019) Enhancement of fuel characteristics of rice husk via torrefaction process. Waste Manag Res. https://doi.org/10.1177/0734242X19838620
35. Odusote JK, Adeleke AA, Lasode OA, Malathi M (2019) Thermal and compositional properties of treated Tectona grandis. Biomass Convers Biorefin. https://doi.org/10.1007/s13399-019-00398-1
36. Aslam U et al (2019) Enhancement of fuel characteristics of rice husk via torrefaction process. Waste Manag Res 37(7):737–745. https://doi.org/10.1177/0734242X19838620
37. Lu X, Xu R, Sun K, Jiang J, Sun Y, Zhang Y (2022) Study on the E ff ect of torrefaction on pyrolysis kinetics and thermal behavior of cornstalk based on a combined approach of chemical and structural analyses. ACS Omega. https://doi.org/10.1021/acsomega.2c00047
38. Jiang S et al (2021) Combining oxidative torrefaction and pyrolysis of phragmites australis: improvement of the adsorption capacity of biochar for tetracycline. Front Energy Res 9. https://doi.org/10.3389/fenrg.2021.673758